

ORIGINAL ARTICLE

Monolithic growth of partly cured polydimethylsiloxane thin film layers

Liyun Yu and Anne Ladegaard Skov

The demand for monolithic structures in many applications has increased to enable more reliable and optimized performances such as for dielectric electroactive polymers (DEAPs). For the layers of the elements to grow efficiently together, it is first of all required that the layers adhere together to enable interlayer crosslinking reactions either by application of an adhesion promoter or by ensuring that there are reactive, complementary sites available on the two surfaces. Polydimethylsiloxane (PDMS) is a widely used polymer for DEAPs. In this work, two-layered PDMS films are adhered together at different curing times. The monolithic films are investigated by rheology, scanning electron microscope, mechanical testing, dielectric relaxation spectroscopy, thermal gravimetric analysis (TGA) and differential scanning calorimetry (DSC). The morphology, mechanical and dielectric properties, as well as thermal stabilities of the bilayer elastomer films are observed to change with the curing time of the monolayers before lamination. The objective of this work is to create adhesion of two layers without destroying the original viscoelastic properties of the PDMS films, and hence enable, for example, adhesion of two microstructured films which is currently a crucial step in the large-scale production of DEAPs.

Polymer Journal (2014) 46, 123–129; doi:10.1038/pj.2013.72; published online 28 August 2013

Keywords: adhesion; crosslinking; dielectric electroactive polymers; monolithic; polydimethylsiloxane

INTRODUCTION

Modern engineering systems are increasingly being produced from components that combine two or more materials for enhanced performance.^{1,2} A complete monolithic structure is made of one single part and has been used so far for multiple layer elastomeric valves, pumps, actuators, etc.^{3,4} Recent investigations from both a technological and a fundamental point of view show that the interfacial bonding strength has a profound influence on the failure of dissimilar or composite materials.⁵ Adhesion is the interatomic and intermolecular interaction at the interface of two surfaces.⁶ The use of adhesion science and technology provides many attractive solutions to the problems in contemporary industrial culture.⁷ The many well-known advantages of adhesion over other joining technologies are better stress distribution over the joint area,^{8,9} the ability to join dissimilar materials,¹⁰ the ability to join thin materials,¹¹ ease of manufacture,¹² reduction in weight,¹³ and often an improved esthetical appearance.¹⁴

Adhesion may be altered using specific physic-chemical properties of the corresponding surface material.¹⁵ It is a complex and multifaceted phenomenon, which is controlled by various factors such as the loading rate, interface toughness, temperature and geometric and molecular properties.¹⁶ The recent adhesion literature contains studies of three main adhesion mechanisms: mechanical coupling, molecular bonding and thermodynamic adhesion.¹⁷ Molecular

bonding (for example, crosslinking) is the most widely accepted mechanism for explaining adhesion between two surfaces in close contact.^{18,19}

Silicones (polydimethylsiloxane (PDMS)) are widely used in electroactive polymer (EAP) formulations due to their favorable electro-mechanical properties. Dielectric electroactive polymers (DEAPs) that consist of an elastomer film with deposited electrodes on both sides have lately gained increased interest as materials for actuators, generators and sensors.²⁰ Most attempts to improve their electro-mechanical properties so far are based on blending or mixing of large particles or molecules into the matrix. This has the disadvantage that agglomeration between particles can occur, thus leading to local regions with different properties compared with the remaining composite.

The hydrosilylation reaction is the addition of a hydridosiloxane or a hydridosilane group to an unsaturated end-capped vinyl group in siloxane elastomers or alternatively polypropylene oxide networks,²¹ catalyzed by a transition metal catalyst such as Speier's catalyst or Karstedt's catalyst in commercially available liquid silicone rubbers or room temperature vulcanizing silicones.²² The two components are Part A: vinyl end-capped PDMS and crosslinker and Part B: PDMS and catalyst. The position and concentration of both vinyl (-CH=CH₂) and hydride (-Si-H) groups along the siloxane backbone decide the nature of the elastomeric network.²³

An important signature during the crosslinking is the so-called gel point. It characterizes the state when a 3-dimensional network of crosslinked molecules is formed.²⁴ Therefore, it characterizes the transition from a viscoelastic liquid to a viscoelastic solid. It is well known that the crosslinking adhesion between two elastomeric sheets can be controlled by the crosslinking density in the interface.²⁵ In this work, monolithic PDMS films were synthesized by adhering two partly cured films together. The interfacial crosslinking density of the double-layered films was evaluated by means of rheology. This method gives information not only on the time-dependent crosslinking, but also on the development of the viscoelastic properties with time. Such results are of great advantage as the processing of the elastomer requires detailed knowledge of the viscoelastic behavior and the crosslinking kinetics because shaping and crosslinking are often intended to be carried out in one step.²⁶ This means that shaping is limited by the material attaining a gel-like state. The objective of the present work is to study the effect of the time, at which the actively curing films are laminated, on the interface structure, the viscoelastic properties, tensile forces, elongation rates, dielectric performances and thermal stabilities of the resulting bilayers.

EXPERIMENTAL PROCEDURE

Materials

PDMS (DMS-V35) ($M_w = 49\,500\text{ g mol}^{-1}$) and tetrakis(dimethylsiloxy)silane (4-functional (4f) crosslinker) ($M_w = 328\text{ g mol}^{-1}$) were purchased from Gelest Inc., Frankfunt am Main, Germany. The catalyst platinum cyclovinylmethyl-siloxane complex (511) was supplied by Hanse Chemie AG., Geesthacht, Germany. FEP fluorocarbon film was obtained from DuPont, Wilmington, DE, USA.

Preparation of films

The films to be adhered together were prepared by a hydrosilylation reaction, where the linear vinyl-terminated PDMS chains were crosslinked with the 4f hydride crosslinker, and the reaction was catalyzed by a platinum catalyst. PDMS, 4f crosslinker and catalyst were mixed uniformly using a Speed Mixer (DAC 150 FVZ; Hauschild Co., Hamm, Germany) at 2000 r.p.m. for 2 min. The homogeneity of the samples was ensured by taking out three samples from the bottom, top and middle of the reaction mixture and running infrared spectroscopy on the samples. The uniform mixture was cast on the FEP foil using a casting knife with a gap of 0.5 or 1 mm. The stoichiometric imbalance (r) of the films was 1. The crosslinking reaction taking place between the reactive groups of 4f crosslinker and PDMS (that is, hydride (-Si-H) and vinyl (-CH=CH₂)) is presented in Figure 1. The stoichiometric imbalance r is given by Equation (1), which is the ratio between the reactive groups of the crosslinker and PDMS:²⁰

$$r = \frac{[\text{hydride}]}{[\text{vinyl}]} = \frac{f \times \frac{m_{\text{crosslinker}}}{M_{\text{crosslinker}}}}{2 \times \frac{m_{\text{PDMS}}}{M_{\text{PDMS}}}} \quad (1)$$

where f is the functionality of the crosslinker ($f=4$), $M_{\text{crosslinker}}$ is the molecular weight of crosslinker (328 g mol^{-1}), M_{PDMS} is the molecular weight of PDMS ($49\,500\text{ g mol}^{-1}$), $m_{\text{crosslinker}}$ is the mass of crosslinker in the mixture and m_{PDMS} is the mass of PDMS polymer in the mixture.

The uncured PDMS films with the thickness of 0.5 mm were used for the adhesion at different curing times according to the rheological curing profile. Figure 2 illustrates where the samples for the adhesion procedure were laminated. The films were left in air to cure for 24 h without any force applied to the two films. After 24 h, the films were fully cured according to rheological curing profile.

Characterization

Rheological measurements. The rheological measurements on the crosslinking behavior were carried out in an inert nitrogen atmosphere using a strain-controlled shear rheometer (AR2000; TA instruments Rheology Division, New Castle, DE, USA) set to a controlled strain mode with 2% strain, which was

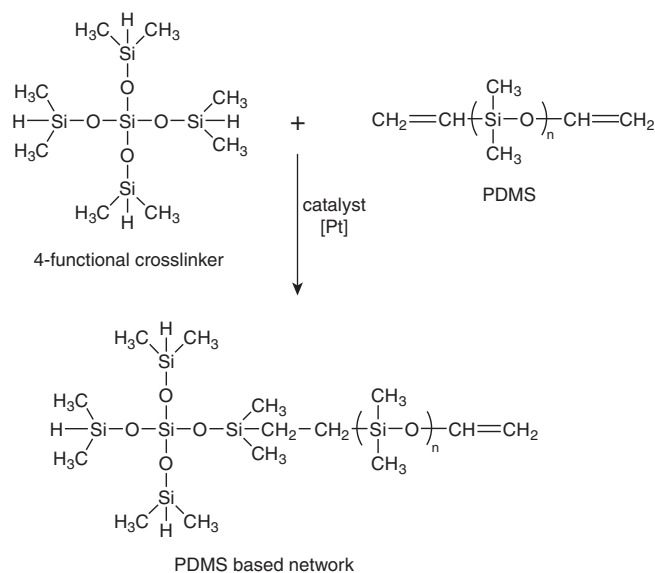


Figure 1 Schematic of the crosslinking reaction between polydimethylsiloxane (PDMS) and 4f crosslinker.

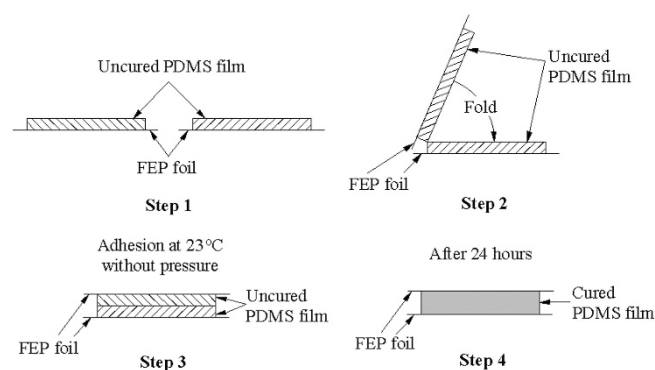


Figure 2 Adhesion procedure of the double-layered polydimethylsiloxane (PDMS) films.

ensured to be within the linear regime of the material based on an initial strain sweep test. Time-resolved dynamic-mechanical experiments of the PDMS mixture were performed at a constant frequency of 1 Hz applying parallel-plate geometry of 25 mm in diameter and a gap of 0.5 mm at 23 °C. The linear viscoelastic data of the PDMS films were measured with parallel-plate geometry of 25 mm in diameter at 23 °C. The linear viscoelastic diagrams were obtained from frequency sweeps from 100 to 0.01 Hz.

Morphology observation. The morphology of the films was examined by a scanning electron microscopy (FEI Inspect S, Hillsboro, OR, USA). The films were initially immersed into liquid nitrogen for a few minutes, then broken and deposited on a copper holder. All samples were coated with gold under vacuum before testing.

Mechanical tests. 180° peel tests were done for all the double-layered films on a material test machine (Zwick Z010, Ulm Germany) at a strain rate of 50 mm min⁻¹ at 23 °C and 60% relative humidity. All the joints were tested three times and then averaged.

Tensile strength and elongations were also measured by the material test machine (Zwick Z010) at a loading velocity of 50 mm min⁻¹ at 23 °C and 60% RH. The reported values are the average value of at least three samples.

Dielectric characterization. Dielectric relaxation spectroscopy was performed on a Novocontrol Alpha-A high performance frequency analyzer (Novocontrol Technologies GmbH & Co. KG, Hundsangen, Germany) operating in the frequency range of 10^{-1} – 10^6 Hz at 23 °C. The diameter of the samples was 25 mm.

Thermal analyses. The thermal stability of films was evaluated by thermal gravimetric analysis (TGA Q500; TA Instruments, USA). The TGA measurements were carried out under a nitrogen atmosphere at a heating rate of $10^\circ\text{C min}^{-1}$ from 23 to 800 °C. Differential scanning calorimetry (DSC Q1000; TA Instruments) measurements were performed on the films from -90 to 200 °C at a heating rate of $10^\circ\text{C min}^{-1}$ under nitrogen atmosphere.

RESULTS AND DISCUSSION

Curing profiles

The dynamic moduli G' and G'' during the isothermal curing at 23 °C are shown in Figure 3. The final value of the storage modulus was labeled as G'_f . The points ($0.1G'_f$, $0.2G'_f$, $0.3G'_f$, $0.4G'_f$, $0.5G'_f$, $0.6G'_f$, $0.7G'_f$, $0.8G'_f$, $0.9G'_f$ and G'_f) at the G' curve correspond to the corresponding values of the time. The partly cured PDMS films with the thickness of 0.5 mm were folded at these different curing times into bilayer laminates, and the samples were labeled as $0.1G'_f$ and so forth. This nomenclature was used to indicate that for $0.1G'_f$ 10% of the final elastic properties were developed at the lamination point.

Elasticity

For any material, the elastic modulus (G') may be defined as the ratio of stress to strain wherein the strain produced by the stress is vanishingly small. Therefore, the 'softer' the material is, the smaller the modulus will be. For crosslinkable materials, an increase in the modulus is also a measure of the increased crosslinking of the materials.²⁷ Figure 4 shows the elastic modulus (G') of the PDMS films as a function of the applied frequency at 23 °C.

The storage modulus G' of the thin single layer PDMS film (0.5 mm) is the lowest and the highest for the thick single layer (1 mm). This can be explained by the findings of Torres *et al.*²⁸ who found that the elastic modulus of a rigid polymer was thickness independent, whereas G' of a more flexible polymer decreased with decreasing thickness. Fedorchenko *et al.*²⁹ suggested that the surface energy became comparable or even larger than the volumetric energy in the thin film. Diaconu *et al.*³⁰ reported that Young's modulus of the polyurethane elastomers increased with thickness from 15 to 110 μm , indicating that in thicker films the phase segregation process into soft and hard domains was more pronounced.

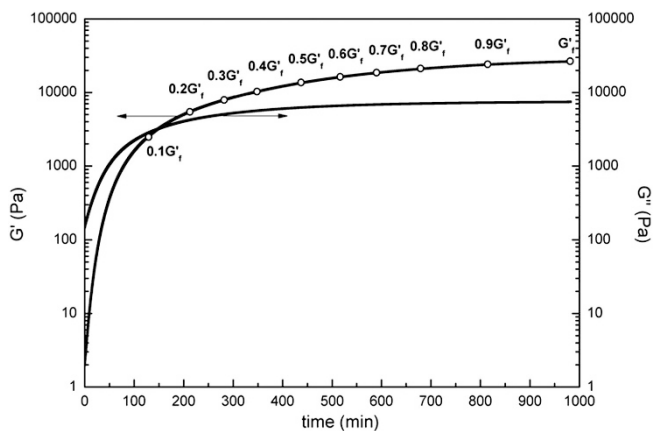


Figure 3 Storage modulus (G') and loss modulus (G'') of the polydimethylsiloxane (PDMS) mixture versus curing time at 23 °C. The points indicate where the different samples are laminated.

Also in Figure 4, the elastic moduli, which are determined from G' at the frequency of 0.01 Hz, are shown as a function of G' at the adhesion time (insert). $0G'_f$ corresponds to the 1 mm single film that would resemble a double-layered film laminated at time 0, which is a sample that cannot be made authentically due to the liquid behavior of the silicones. Before the curing the silicones are liquid and the films are not easily turned upside down and laminated without introduction of significant defects. The influence of interfacial curing time on the elastic modulus of the bilayer films is clear. G' was observed to reach a minimum of $0.3G'_f$ double-layered films. At short interfacial curing times ($0.1G'_f$ and $0.2G'_f$), the G' curves are similar to the thick film (1 mm), which fit the curing profile as shown in Figure 3. The laminating times of $0.1G'_f$ and $0.2G'_f$ are in the proximity of the gel point. At the gel point, the molecular weight distribution is infinitely broad with molecules ranging from the smallest unreacted chain to the infinite continuous structure. The integrated network structures of films ($0.1G'_f$, $0.2G'_f$ and 1 mm) are homogeneous, thereby demonstrating that there is no obvious change in their elastic moduli. In other words, the samples laminated around the gel point clearly become monolithic, even at times slightly exceeding the gelation threshold. Interestingly, G' of the two-layered films gradually increased with the decreasing reaction time at the interface ($0.4G'_f$ – $0.7G'_f$ in Figure 4). This could be ascribed to the slow diffusion or reptation of the inreacted groups to and on the surface such that only the shortest chains will migrate to the surface and cause a shorter distance between crosslinking sites at the surface. However, the unfavorable dynamics for the reaction to proceed at the interface will probably leave a fair amount of inreactive species such that the overall crosslink density of the surface does not exceed the bulk crosslinking density.

Microstructure

The crosslinking reaction takes place between the reactive groups of the linear vinyl-terminated PDMS and 4-functional crosslinkers (that is, vinyl ($-\text{CH}=\text{CH}_2$) and hydride ($-\text{Si}-\text{H}$)).²² A possible structural model of the double-layered films is shown in Figure 5. In Figure 5a, the network structures of the interface and two bulks are alike, and the crosslink density is uniform throughout the whole matrix. This is in good agreement with the data showing that the elastic moduli of

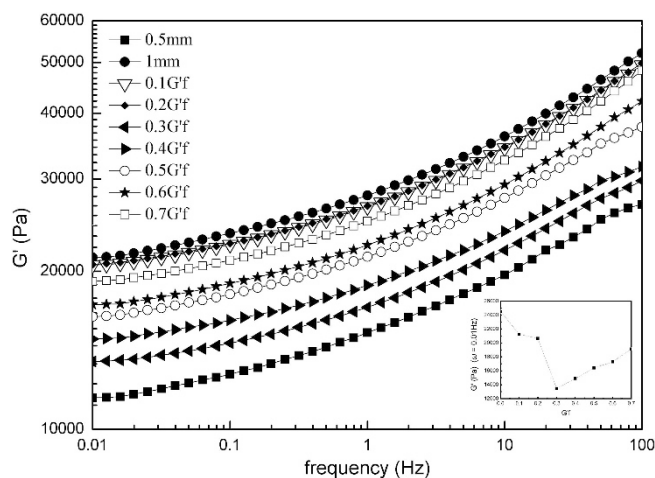


Figure 4 Elastic modulus (G') of polydimethylsiloxane (PDMS) films as a function of applied frequency at 23 °C. G' at $\omega = 0.01$ Hz is also shown as a function of G' at the adhesion time (insert), and $0G'_f$ corresponding to the thick (1 mm) sample.

$0.1G'_f$, $0.2G'_f$ and 1 mm films are similar (Figure 4). After $0.3G'_f$ linear chain segments, partly or non-reacted, are most likely to move to the surface. As seen in Figure 5b, when the interfacial reaction is insufficient, the bonding junctions could not be covered well over the film surfaces and the adhesion is weak, which is proven by the following results of the adhesion strength test. Finally, the interfacial bond failure occurs in the joints. The data fit very well with the data from the rheological characterization. Figure 6 shows the cross-section morphologies of double-layered PDMS films ($0.2G'_f$ and $0.3G'_f$) in different magnifications. There is obvious difference between $0.2G'_f$ and $0.3G'_f$ films. In Figures 6a and b, the interface in the $0.2G'_f$ film is very obscure and discontinuous, which indicates its bulk structure and fits well with the elasticity results. Usually, the existence of air bubbles and defects results in an insufficient adhesion.³¹ In Figures 6c and d the continuous and very thin vertical midlines are the interfaces of the two-layered films ($0.3G'_f$). The tight junction interface is in agreement with the peeling test later, which means that there exists sufficient crosslink bonding at the interface of the $0.3G'_f$ sample to make the joint mechanically invisible and hence to make the bilayer a true monolithic structure.

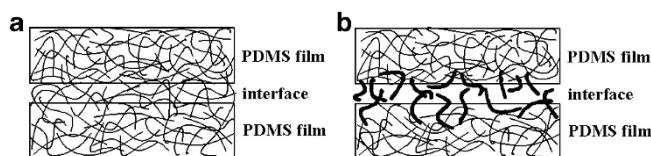


Figure 5 Schematic illustration of the polydimethylsiloxane (PDMS) films with different interfacial structures: (a) interface and bulks with similar network chains ($0.1G'_f$, $0.2G'_f$ and 1 mm films), and (b) interface consisting of dangling short chains ($0.8G'_f$ – G'_f).

Adhesion strength

There are two reactions happening in the two-layered PDMS films. One is that, the liquid PDMS transforms into the solid state. The other is that there exists spontaneous adhesive connection between the two partly cured PDMS layers resulting in an interfacial connection of these two substrates. From experiments, it was found that at a curing temperature of 23°C , the liquid PDMS prepolymer will become more and stickier with increasing curing time up to 148.8 min (the gel point as seen in Figure 3) which is slightly after $0.1G'_f$. During this stage, the bonding strength of the interface becomes very close to that of the native interaction inside the PDMS bulk, demonstrating near-complete monolithic growth between the two parts. After that, PDMS prepolymer will gradually translate into the solid state upon further curing. Once solidification happens, the state transfer can be successfully achieved, but at the same time, the adhesive interaction will become distinct. The adhesion strength of double-layered films was measured by 180° peel test and the results are given in Table 1. The peeling strength for samples ($0.1G'_f$ and $0.2G'_f$) is not reported because rupture during the peel test was experienced which again confirms the monolithic structures of the bilayers. Table 1 indicates that the adhesion force of the non-permanently bonded interfaces increases with increasing curing time at the interlayer. It can be seen that at G'_f , the peeling strength between two PDMS strips is measured to be 1.04 N mm^{-1} , which is very close to that of the native interaction between PDMS and glass.³² Prolonging the interfacial curing time increases the peeling strength significantly. When the curing time reaches $0.3G'_f$, a maximum peeling strength of 3.47 N mm^{-1} is obtained and fracture is found in the PDMS strip rather than at the interface, demonstrating near-complete fusion between the two parts (as shown in Figure 6).

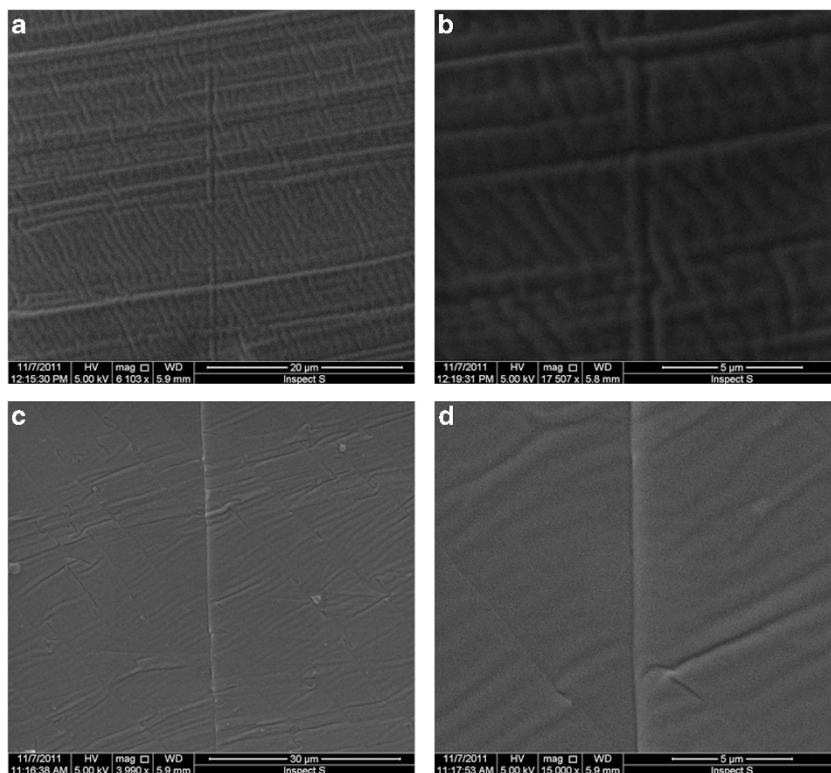
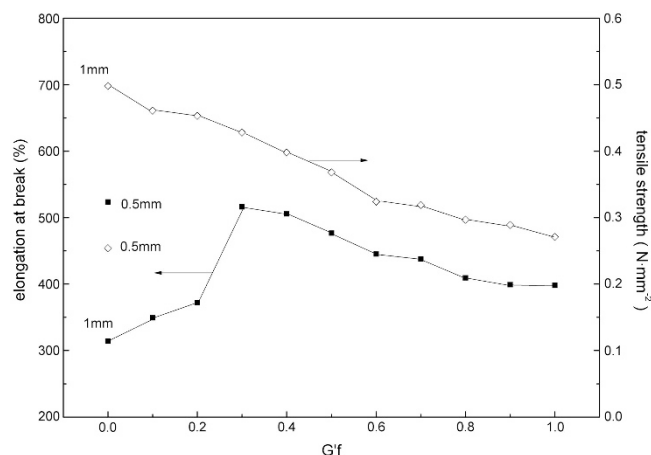


Figure 6 Cross-section morphologies of double-layered polydimethylsiloxane (PDMS) films in different magnifications: (a, b) $0.2G'_f$ and (c, d) $0.3G'_f$.

Table 1 Measurement results of the T-peeling test

No.	$0.3G'_f$	$0.4G'_f$	$0.5G'_f$	$0.6G'_f$	$0.7G'_f$	$0.8G'_f$	$0.9G'_f$	G'_f
Peeling strength (N mm^{-1})	3.47	3.31	3.25	3.21	2.98	2.82	2.79	1.04

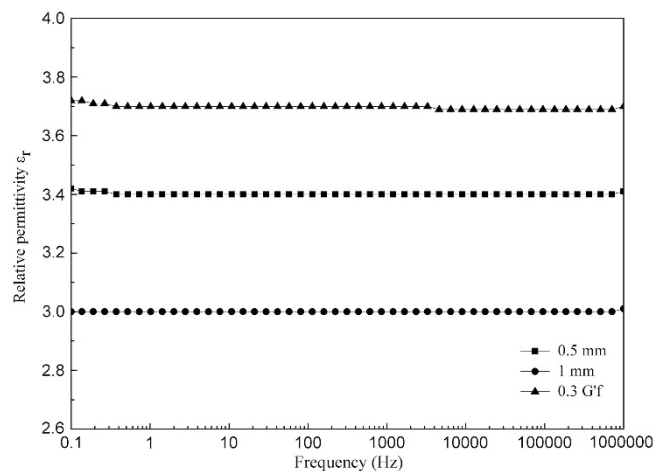

Figure 7 Elongation at break and tensile strength of polydimethylsiloxane (PDMS) films.

Mechanical properties

The results of mechanical strength test including elongation at break and tensile strength are shown in Figure 7. After the tension tests, the stress–strain curves of all the samples were calculated from the automatically recorded raw data. The elongation results fit the elasticity of the films (Figure 4) very well and the explanation has been given before. Typically, reinforcement with soft polymeric chains is accompanied by a decrease in tensile strength.²⁶ This is not the case with the $0.3G'_f$ sample, which retains the high tensile strength (0.428 N mm^{-2}) and even exhibits the largest elongation of the films (516%). The large size distribution of the soft segments at the interface, which formed entanglements, led to the less free-moving structures and thus improved the tensile strength.³³ The $0.3G'_f$ sample was thus chosen in the following studies to compare the dielectric and thermal properties with the single films as the film was recognized both mechanically and morphologically to be very close to monolithic.

Dielectric properties

The relative dielectric permittivity (ϵ_r) indicates the ability of a material to store electric potential energy under the influence of an external electric field. It is known that the permittivity of elastomers can be increased by decreasing the homogeneity of the molecular structure.³⁴ Dielectric spectra were recorded for both single and double-layered films (0.5 mm, 1 mm and $0.3G'_f$) and they are shown in Figure 8. No relaxation in the frequency regime of 0.1 Hz to 1 MHz was recorded, that is, $\epsilon'' \ll \epsilon'$. The relative dielectric permittivities of the three samples were measured to be $\epsilon_r = 3.0$ for the thick film, $\epsilon_r = 3.4$ for the thin film and $\epsilon_r = 3.7$ for the bilayer. The significant increase for the bilayer may be due to the inhomogeneous microstructure at the interface, which leads to the enhancement of interfacial polarization, thus increasing the permittivity ϵ_r . Since Young's modulus E and ϵ_r are closely interrelated, it is very important


Figure 8 Frequency-dependent permittivity spectra of films.

to do a combined optimization between G' and ϵ_r in the elastomers. The lamination process proceeding around or slightly above the gelation threshold seems to be very favorable in context of the desired enhancement of the dielectric permittivity for EAP materials.

Thermal stabilities

Again three different films were investigated, namely the single films of thicknesses 0.5 and 1 mm as well as the double-layered film $0.3G'_f$. As shown in Figure 9a, the $0.3G'_f$ film has the highest thermal decomposition temperature T_d , which is defined as the temperature at which a weight loss of 3% is recorded,³⁵ compared with that of the single PDMS films. The thermal degradation of the single films started at above 410.2°C (0.5 mm) and 417.5°C (1 mm), and the complete decompositions for both these films are observed at around 565°C (0.5 mm) and 603°C (1 mm). However, the degradation of the $0.3G'_f$ sample began at around 426.8°C , ~ 10 degrees later than for the two monolayers, and ended at 610.2°C again later than for the monolayers. This indicates a slightly better thermal stability of the laminated film, probably due to the strongly bonded three-dimensional interfacial network that hindered the degradation of molecular chains produced by the siloxane bond interchange reaction.³⁶ The TGA used in this study has previously proven to be able to record the presence of components in even % range and we therefore believe that the measurements are not experimental artifacts but rather very reliable measurements showing the presence of a thermal stabilizing interface.

Figures 9b and c illustrate the DSC curves of the three different films. In the cooling curves (Figure 9b) and heating curves (Figure 9c), the exothermic peaks (crystallization point T_c) and endothermic peaks (melting point T_m) were observed, respectively.³⁷ Both properties are very similar for the three films but there are, however, slight changes confirming the previously discussed results obtained from rheology. Both the crystallization and melting points of thick film (1 mm) are lowest ($T_c -76.9^\circ\text{C}$ and $T_m -44.4^\circ\text{C}$), which is in agreement with the data from Figure 4 where it was concluded that the 1 mm film was the film with the highest crosslink density. Moreover, both the highest crystallization and melting points for the samples (-75.1°C and -42.3°C , respectively) were recorded for the laminated film ($0.3G'_f$). This proves that there is good incorporation of PDMS within the soft long chains at the interlayer, which potentially could reinforce the crystallization and melting temperatures of the elastomers.³⁸

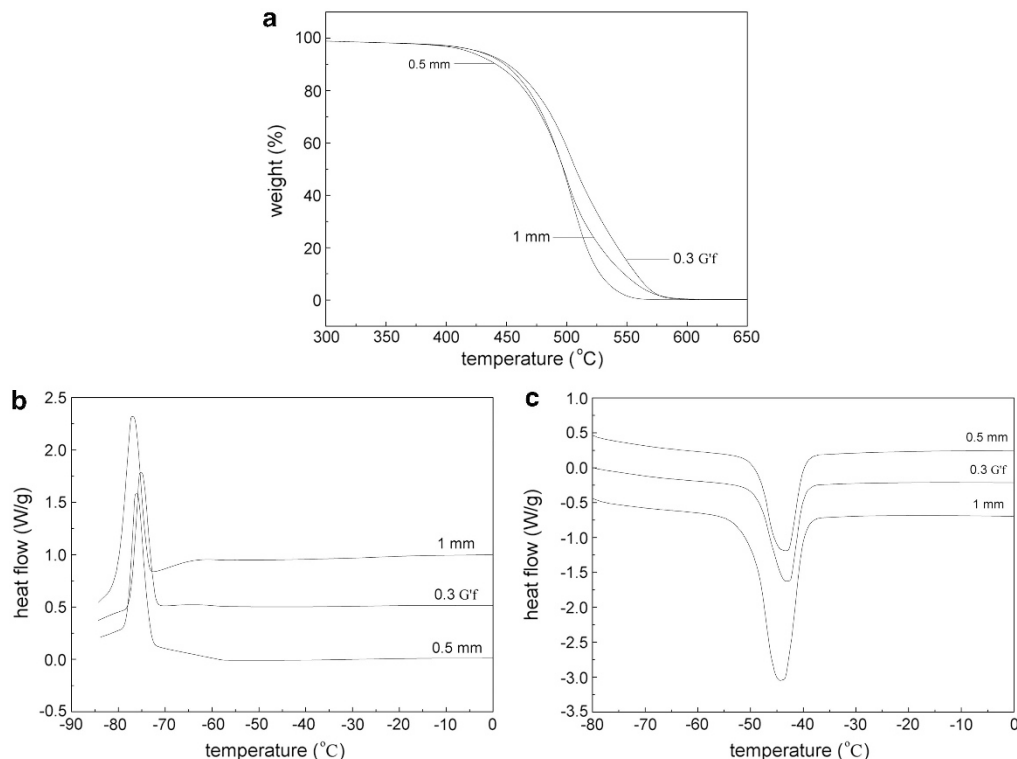


Figure 9 Thermal gravimetric analysis (TGA) and differential scanning calorimetry (DSC) thermograms of films. (a) TGA: 0.5 mm, T_d 410.2 °C; 1 mm, T_d 417.5 °C; 0.3G'_f, T_d 426.8 °C. (b) DSC: 0.5 mm, T_c -76.0 °C; 1 mm, T_c -76.9 °C; 0.3G'_f, T_c -75.1 °C. (c) DSC: 0.5 mm, T_m -43.3 °C; 1 mm, T_m -44.4 °C; 0.3G'_f, T_m -42.3 °C.

CONCLUSIONS

Double-layered PDMS films were prepared by lamination of two partly cured films at different curing times. The viscoelastic behavior, microstructure and mechanical strength, as well as dielectric permittivity and thermal properties of the monolithic films were shown to vary with the time of lamination. For growth of a true monolithic structure, the lamination process had to be done before the gelation threshold. However, for EAP uses the lamination performed slightly above the gelation threshold, namely at the time where the monolayer films had gained 30% of the final mechanical strength, was extremely favorable, since the resulting bilayer was mechanically identified as monolithic and the scanning electron microscopy pictures revealed a very weak surface only, combined with a significant increase in the dielectric permittivity due to this interface. In other words, it means that the lamination process for EAP bilayers can actually be used as a process to improve the overall performance of the EAP.

ACKNOWLEDGEMENTS

We gratefully acknowledge the financial support from the Danish National Advanced Technology Foundation. Michael Daniel Junker, Danfoss PolyPower, is acknowledged for his help with the mechanical tests.

- Benslimane, M., Tryson, M. J., Oubak, J. & Kiil, H. E. in *Electroactive Polymer Actuators and Devices (EAPAD): 7976 797601-1 797601-13*. Proc. of SPIE (eds Yoseph, B. C. & Federico, C.) (San Diego, CA, USA, 2011).
- Benslimane, M., Kiil, H. E. & Tryson, M. J. in *Electroactive Polymer Actuators and Devices (EAPAD): 7642 764231-1 764231-11*, Proc. of SPIE (ed. Yoseph, B. C.), (San Diego, CA, USA, 2010).

- Unger, M. A., Chou, H. P., Thorsen, T., Scherer, A. & Quake, S. R. Monolithic microfabricated valves and pumps by multilayer soft lithography. *Science* **288**, 113–116 (2000).
- Sansiñena, J. M., Gao, J. & Wang, H. L. High-performance, monolithic polyaniline electrochemical actuators. *Adv. Funct. Mater.* **13**, 703–709 (2003).
- Xu, L. R., Sengupta, S. & Kuai, H. C. An experimental and numerical investigation of adhesive bonding strengths of polymer materials. *Int. J. Adhes. Adhes.* **24**, 455–460 (2004).
- Poisson, C., Hervais, V., Lacrampe, M. F. & Krawczak, P. Optimization of PE/binder/PA extrusion blow-molded films. II. Adhesion properties improvement using binder/EVA blends. *J. Appl. Polym. Sci.* **101**, 118–127 (2006).
- Öchsner, A., Stasiek, M., Mishuris, G. & Grácio, J. A new evaluation procedure for the butt-joint test of adhesive technology: determination of the complete set of linear elastic constants. *Int. J. Adhes. Adhes.* **27**, 703–711 (2007).
- Comyn, J. in *Handbook of Adhesives and Sealants 2* (ed. Cognard, P.) (Elsevier, Amsterdam, Netherlands, 2006).
- Haghani, R., Emrani, M. A. & Klinger, R. Stress distribution in adhesive joints with tapered laminates-effect of tapering length and material properties. *J. Compos. Mater.* **44**, 287–302 (2010).
- Kumar, P., Singh, R. K. & Kumar, R. Joining similar and dissimilar materials with GFRP. *Int. J. Adhes. Adhes.* **27**, 68–76 (2007).
- Kadioglu, F. & Souni, M. E. Use of thin adherends in adhesively bonded joints under different loading modes. *Sci. Technol. Weld. Joining* **8**, 437–442 (2003).
- Okuzu, T. & Kuwata, H. *Easy adhesion polyamide film and production method therefor*. US, 2012/0003440 A1, 2012-01-05.
- Watson, C. in *Handbook of Adhesion 138* (ed. Packham, D. E.) (Wiley, Hoboken, NJ, USA, 2005).
- Packham, D. E. Adhesive technology and sustainability. *Int. J. Adhes. Adhes.* **29**, 248–252 (2009).
- Loher, S. & Stark, W. J. Rapid production of micropatterned surfaces using a fluid dynamical instability. *Polym. Eng. Sci.* **46**, 1541–1547 (2006).
- Kulmi, U. & Basu, S. A molecular dynamics study of the failure modes of a glassy polymer confined between rigid walls. *Modell. Simul. Mater. Sci. Eng.* **34**, 948–968 (2009).
- Awaja, F., Gilbert, M., Kelly, G., Fox, B. & Pigram, P. J. Adhesion of polymers. *Prog. Polym. Sci.* **34**, 948–968 (2009).
- Kinloch, A. J. The science of adhesion. I. Surface and interfacial aspects. *J. Mater. Sci.* **15**, 2141–2166 (1980).
- Adnan, A. & Sun, C. T. Effect of adhesive thickness on joint strength: a molecular dynamics perspective. *J. Adhes.* **84**, 401–420 (2008).

- 20 Skov, A. L., Bejenariu, A. G., Bøgelund, J., Benslimane, M. & Egede, A. D. in *Electroactive Polymer Actuators and Devices (EAPAD): 8340 83400M-1 83400M-10. Proc. of SPIE* (ed. Yoseph, B. C.) (San Diego, CA, USA, 2012).
- 21 Jensen, M. K., Bach, A., Hassager, O. & Skov, A. L. Linear rheology of cross-linked polypropylene oxide as a pressure sensitive adhesive. *Int. J. Adhes. Adhes.* **29**, 687–693 (2009).
- 22 Bejenariu, A. G., Rasmussen, H. K., Skov, A. L., Hassager, O. & Frankaer, S. M. Large amplitude oscillatory extension of soft polymeric networks. *Rheol. Acta* **49**, 807–814 (2010).
- 23 Bejenariu, A. G., Yu, L. Y. & Skov, A. L. Low moduli elastomers with low viscous dissipation. *Soft Matter* **8**, 3917–3923 (2012).
- 24 Winter, H. H. & Chambon, F. Analysis of linear viscoelasticity of a cross-linking polymer at the gel point. *J. Rheol.* **30**, 367–382 (1986).
- 25 Lin, P. C., Vajpayee, S., Jagota, A., Huid, C. Y. & Yang, S. Mechanically tunable dry adhesive from wrinkled elastomers. *Soft Matter* **4**, 1830–1835 (2008).
- 26 Wolff, F., Kugler, C. & Münstedt, H. Time- and temperature-dependent crosslinking behavior of a silicone resin. *Rheol. Acta* **51**, 71–80 (2012).
- 27 Ramesh, K., Tock, R. W., Narayan, R. S. & Vallabhan, C. V. G. Property evaluation of silicone elastomers used in tension-adhesion joints. *J. Mater. Sci. Lett.* **14**, 964–967 (1995).
- 28 Torres, J. M., Wang, C. Q., Coughlin, E. B., Bishop, J. P., Register, R. A., Riggleman, R. A., Stafford, C. M. & Vogt, B. D. Influence of chain stiffness on thermal and mechanical properties of polymer thin films. *Macromolecules* **44**, 9040–9045 (2011).
- 29 Fedorchenko, A. I., Wang, A. B. & Cheng, H. H. Thickness dependence of nanofilm elastic modulus. *Appl. Phys. Lett.* **94**, 152111-1–152111-3 (2009).
- 30 Diaconu, I., Dorohoi, D. O. & Ciobanu, C. Electromechanical response of polyurethane films with different thickness. *Rom. J. Phys.* **53**, 91–97 (2008).
- 31 Cho, S. M., Hong, J. H., Kim, Y. T. & Lee, S. D. Adhesive-transfer bonding technique for flexible liquid crystal displays with high mechanical stability. *Mol. Cryst. Liq. Cryst.* **513**, 1–8 (2009).
- 32 Aarash, Y. N. S. & Cristina, M. A vapor-assisted method for adhering polydimethylsiloxane and glass. *Lab. Chip.* **10**, 250–253 (2010).
- 33 Delebecq, E., Hermeline, N., Flers, A. & Ganachaud, F. Looking over liquid silicone rubbers: (2) Mechanical properties vs network topology. *ACS Appl. Mater. Interfaces* **4**, 3353–3363 (2012).
- 34 Sahoo, B. P., Naskar, K. & Tripathy, D. K. Conductive carbon black-filled ethylene acrylic elastomer vulcanizates: physico-mechanical, thermal, and electrical properties. *J. Mater. Sci.* **47**, 2421–2433 (2012).
- 35 Yu, L. Y., Xu, Z. L., Shen, H. M. & Yang, H. Preparation and characterization of PVDF-SiO₂ composite hollow fiber UF membrane by sol-gel method. *J. Membr. Sci.* **337**, 257–265 (2009).
- 36 Patwardhan, S. V., Taori, V. P., Hassan, M., Agashe, N. R., Franklin, J. E., Beaucage, G., Mark, J. E. & Clarson, S. J. An investigation of the properties of poly(dimethylsiloxane)-bioinspired silica hybrids. *Eur. Polym. J.* **42**, 167–178 (2006).
- 37 Kuo, A. C. M. in *Polymer Data Handbook*, 2nd edn (ed. Mark, J. E.) 547 (Oxford University Press, Oxford, UK, 2009).
- 38 Rochery, M., Vroman, I. & Lam, T. M. Incorporation of poly(dimethylsiloxane) into poly(tetramethylene oxide) based polyurethanes: the effect of synthesis conditions on polymer properties. *J. Macromol. Sci. Pure Appl. Chem.* **40**, 321–333 (2003).